

Modelling of degradation process of electrical insulation systems due to inverter pulses

Abstract. In-service stresses are the cause of progressive degradation of electrical insulation systems. The assessment of intensity and dynamics of these processes which are, among others, consequence of local working electric field strength is usually performed at sinusoidal voltage. However, in applications where power electronics converters are used the voltage stress has usually a form of fast switching pulses composing of repetitive sequences. Special problems for Pulse Width Modulation (PWM) driven induction motors arise from overvoltages and partial discharges (PD) in insulating systems of feeding cables and motors. The PWM waveforms produce complex overvoltages that stress the insulation more severely than sinusoidal voltage waveforms. The overvoltages form trains of pulses with very short rise times. Such conditions have essential influence on inception and activity of partial discharges in insulation systems. Selected aspects of these problems are presented in the paper: the numerical simulations of electric stress in coil-to-coil insulation of stator windings, the influence of the pulsed voltages modelling the PWM sequences, and the experimental results of PD in model twisted pair (TP) samples.

Streszczenie. Narażenia eksploatacyjne są powodem postępującej degradacji elektrycznych układów izolacyjnych. Ocena intensywności i dynamiki tych procesów, będących m.in. konsekwencją lokalnego, roboczego natężenia pola elektrycznego jest zwykle prowadzona dla napięcia sinusoidalnie zmiennego. W aplikacjach, w których stosowane są energoelektroniczne układy przekształtnikowe narażenia napięciowe mają formę impulsów szybkozmiennych, tworzących powtarzalne sekwencje. Szczególne problemy powstają w układach napędowych silników indukcyjnych z modulacją szerokości impulsów (PWM), a związane są one z przepięciami oraz wyładowaniami niepełnymi (wnz) w izolacji kabli zasilających oraz silników. Przebiegi PWM wytwarzają złożone przepięcia, które narażają izolację w większym stopniu niż napięcia przemienne. Przepięcia tworzą ciągi impulsów o bardzo krótkich czasach narastania, co ma zasadniczy wpływ na powstawanie i aktywność wyładowań niepełnych w układach izolacyjnych. Artykuł przedstawia wybrane aspekty tych problemów: symulacje numeryczne naprężeń elektrycznych izolacji międzyzwojowej, wpływ napięć impulsowych modelujących sekwencje PWM oraz wyniki badań eksperymentalnych wnz w próbkach modelowych typu para skręcona (TP). (Modelowanie procesów degradacji układów elektroizolacyjnych wywołanych impulsami inwertera).

Keywords: electrical insulation systems, degradation processes, partial discharges, PWM voltages

Słowa kluczowe: układy izolacyjne, procesy degradacji, wyładowania niepełne, napięcia PWM

doi:10.12915/pe.2014.10.22

Introduction

The inverter drives based on Pulse Width Modulation (PWM) technique are the most common type of inverter drives used for control of electric machines work. A general scheme of motor control with the PWM inverter drive is presented in Figure 1. The pulsed output voltage is applied from PWM drive to the motor terminals by a feeding cable, which for actual PWM pulses parameters for the most cases can be treated as transmission line [1]. In those drives the sequence control unit produces pulse-width modulated train of voltage pulses with slew rate up to $100 \text{ kV} \cdot \mu\text{s}^{-1}$ and repetition rate even up to 100 kHz. In consequence large spikes, overshoots and oscillations could be observed on motor terminals. Electrical stresses caused by generated supply voltage distortions often lead to partial discharges, faster degradation of the insulation system, its unexpected breakdown, and failure of electrical machine.

The types of insulating systems of electrical machines

The paper is concerned to random wound stator windings insulation system, where the magnet wire is round and the arrangement between the turns is not defined (i.e. random).

The main criterion for classification of winding insulation is related to assessment of PD activities during the lifetime and it refers to the random-wound and form-wound stator windings. According to IEC TS 60034-18-41 [2] the insulation systems of electrical machines fed by voltage inverters are divided into two types:

- Type I** systems which are not expected to experience PD activity in their service,
- Type II** systems which are expected to withstand PD activity throughout their service lifetime.

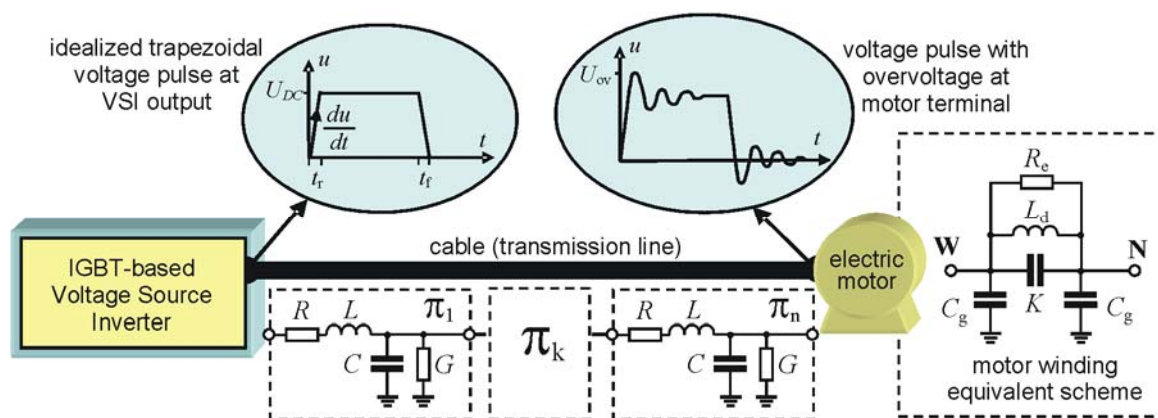


Fig.1. Pulse voltages in single-phase inverter-cable-motor setup: R , L , C , G – parameters of transmission line model, L_d – phase inductance, C_g – distributed ground capacitance, R_e – loss resistance, K – input winding capacitance; U_{DC} – dc-link voltage, U_{ov} – over-voltage crest value, du/dt – voltage slew rate, VSI – Voltage Source Inverter

Machines with a rated voltage:

- to 700 V_{rms} may have either Type I or type II windings,
- above 700 V_{rms} the winding insulation is usually type II.

During the exploitation, the electrical stresses will be created in the following locations in the insulating system (Fig.2): between conductors in different phases or phase-to-phase (U_{PP}), between turn-to-turn (U_{CC}), between a conductor and ground (U_{PG}).

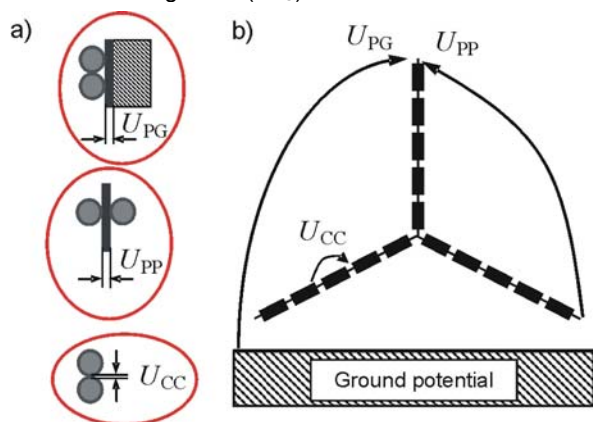


Fig.2. Electrical stresses of motor insulating system: a) details of insulation system of inverter fed motor b) voltages for star connected motor: U_{PP} – phase-to-phase voltage, U_{CC} – conductor-to-conductor voltage, U_{PG} – phase-to-ground voltage

The elements of inverter fed motor insulation system are exposed to repetitive short rise time voltage impulses with significant amplitude. The electric stress is defined by the peak voltages and the basic stressing parameter is the peak-to-peak voltage. It means that the unipolar voltage produces the same stress as a bipolar voltage having a peak-to-peak voltage of the same value. This problem was recognized as first by Bonnet [3] and Person [4], who have recognized that switching devices as IGBT used in PWM converters create the high amplitude voltage impulses at the motor terminals.

For modelling of random-wound windings, the samples called *twisted-pair* (TP) [5] made of magnet wires with different diameters are used. Twisted-pair samples are composed of two enamel-coated together twisted copper wires. According to IEC standard [6] the normalized number of twists t_s on a nominal sample length l equal to 125 mm ranges from 3 – for enamelled wire nominal diameter between 2.15 mm to 3.5 mm to 16 twists – for enamelled wires with a diameter from 0.35 mm to 0.5 mm.

Partial discharges in motor insulation

The degradation mechanism in insulating systems at PWM inverter-fed driver is not the same as for sinusoidal frequency 50/60 Hz. The aging processes, as a result of PD activity, are accelerated by:

- presence of repetitive overvoltages,
- space charge injection in insulation – depending also on various PWM sequences,
- high repetition rate of PD pulses,
- high voltage slew rate (dU/dt).

Theoretically, at semi-square voltages, partial discharges should occur only at a rising and falling slope and vanish during the voltage plateau. The PD intensity should be related to du/dt . However, as shown by many researchers, the PD occurs in the whole voltage period [7, 8, 9], also when $U = \text{const}$. This necessitates a further recognition of the PD mechanism in insulation systems subjected to *PWM*-based drives.

The whole stator winding is resin impregnated. The

resin penetrates and fills the space between wires and stator slots in order to increase the dielectric capability, thus increasing the level of PD inception. The accumulated moisture and contaminants can promote tracking and deterioration, leading to failure. Tracking failures are caused by small partial discharges, which develop localised heating and cause chemical decomposition of any weak insulation barrier. Arcs of relatively high currents develop additional heating, which carbonizes the resin surface. Hence, the need for diagnosing stator windings is twofold:

- already during the manufacturing process the magnet wire coated insulation may be damaged, causing galvanic short circuits, and leading to turn-to-turn / phase-to-phase faults (Fig.3a). Imperfect resin impregnation may result in voids formation and partial discharge development (Fig.3b),
- during operation environmental conditions and mechanical stress, especially vibrations may lead to the insulation degradation. *PWM*-controlled motors might be subjected to an additional stress related to high voltage peaks, which can deteriorate the insulation system. The high electric field between wires in the slot or in the end winding section might start ionization and formation of corona (Fig.3c), which can lead to chemical damage and thermal hot spots.

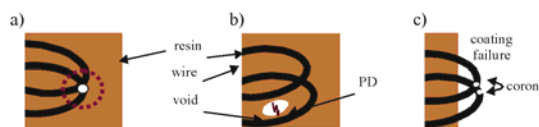


Fig.3. Turn-to-turn faults: a) electrical short-circuits, b) void between magnet wires and internal PD, c) magnet wire insulation failure and corona

The insulation failure occurs when the magnitude and rise time of the repetitive transient voltage stress exceeds the withstand capability of the insulating system (Fig.4). The breakdown of insulation most commonly occur at the highest voltage stress spot, i.e. the first turn of the line end coil to the last turns of the coil group as well as in the end winding region, where wires from different coils can come into contact.

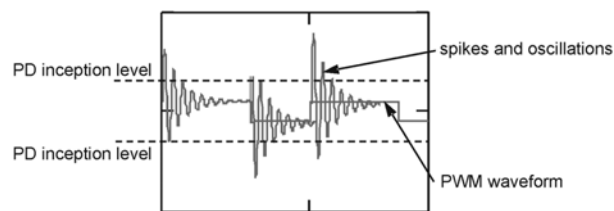


Fig.4. Supply voltage of *PWM* driven motor with overvoltages

The overvoltage stresses can be analyzed at semi-square voltage with a specified rise time t_r , and the overvoltage magnitude U_{ov} depends on the steepness of the semi-square voltage as illustrated in Figure 5. In PD model for such voltage stimulus the rise time t_r is equal to:

$$(1) \quad t_r = \frac{U_{ov}}{tg\alpha}$$

The occurrence of partial discharges depends on inception voltage U_{ci} with respect to the value of U_{ov} and is triggered when $U_{ci} < U_{ov}$ (Fig.5), whereas the discharge intensity and their development also depends on the extinction voltage U_{ce} . The attributes describing the PD sources depend on the ratio U_{ce} / U_{ci} , just like at sinusoidal voltage, and additionally on the rise time t_r .

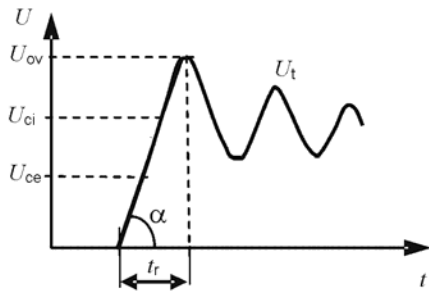


Fig.5. Definition of overvoltage parameters

The factors affected the PD at impulse voltage are: voltage, frequency and pulse rise/fall time. The voltage rise time has special impact on the initiation conditions and on the inception voltage U_i of PD (Fig.6).

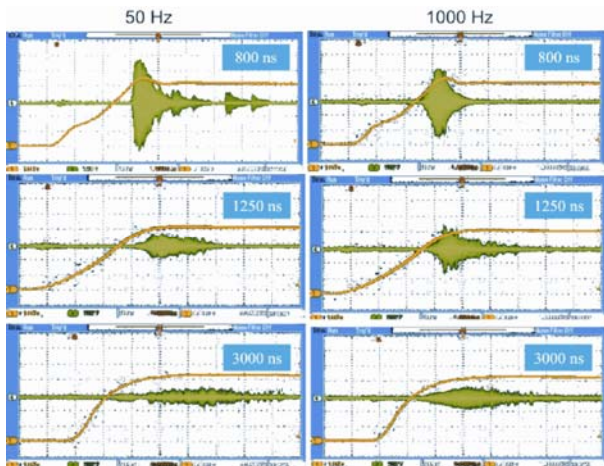


Fig.6. PD pulses acquired in samples of thermosetting insulation for 50 Hz (left) and 1000 Hz (right) and for three rise-time parameters 800-1250-3000 ns (in the case of 3000 ns the time scale is 2 μ s/div otherwise 400 ns/div) [10]

PD pulses acquisition at semi-square voltages

Classic methods of PD detection described in IEC-60270 [11] refer to measurements performed in the frequency range up to 1 MHz and are not useful for voltages with high slew rate, due to frequency spectrum overlapping.

Thus, in the case of PD measurements at semi-square voltages (e.g. generated by IGBT inverter) other specific detection methods operating in *VHF/UHF* range should be applied [12]. In the presented experiments three different types of detectors have been used for PD pulse acquisition: 1) *E*-field detector with 350 MHz amplifier connected to HP-8591E spectrum analyzer, 2) Rogowski coil, and 3) non-inductive resistors. Electric signals from detectors were digitalized and registered by oscilloscopes with implemented DPO function (*Digital Phosphor Oscilloscope*) TDS784D or DPO2014 (Tektronix). The challenge in this kind of experiment, performed at fast stimulus is to separate the PD pulse from the pulses interfering due to HV modulator switching, as shown in Figure 7a. The narrow spike is the PD pulse, however charging current is also detected on wideband resistor. A single PD event, with 6 ns FWHM value (*Full Width at Half Maximum*), is observed in Figure 8. Determination of PDIV (*Partial Discharge Inception Voltage*) under impulse voltages at a level just above ionisation threshold is difficult to monitor precisely because of transient development of ionisation. Acquisition of PD signals in DPO mode for the semi-square voltage (Fig.8b) shows its appearance after the time lag on the rising slope of voltage pulse. The results confirm high

repeatability of pulse voltage and stochastic nature of PD manifested by blurring of amplitude and time location.

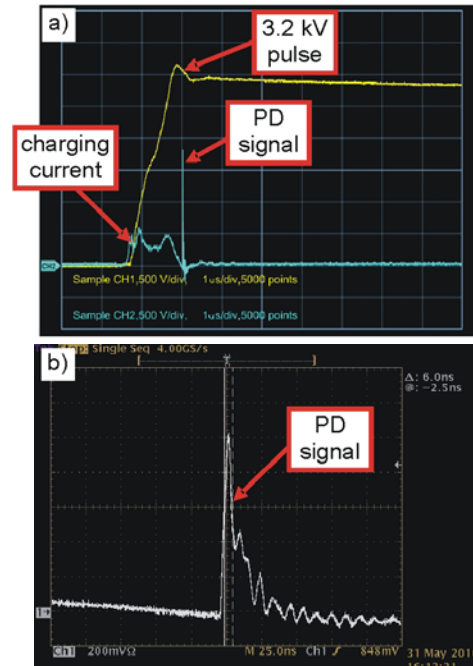


Fig.7. Semi-square voltage and current signal detected on 50 Ω resistor – time scale 1 μ s/div (a) and individual PD pulse registered with 4 GHz sampling frequency (25 ns/div) (b)

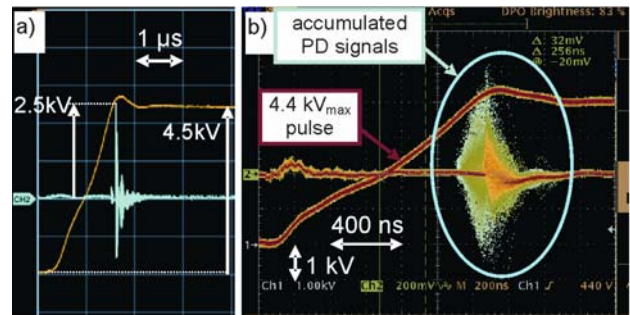


Fig.8. Partial discharges in thermosetting insulation sample for pulse voltage close to inception voltage. Acquisition of semi-square voltage and PD signal from Rogowski coil: a) single-shot acquisition by DPO2014, b) result of 3075 accumulations in DPO mode by TDS784D oscilloscope

PD measurements in model insulation systems

The TP samples have been used for studying the PD phenomena in enameled wires as a substitute of the motor winding. The twisted-pair of TP sample can be regarded as a pair of enameled wires being in contact (Fig.9a) or separated by a micro-air gap g (Fig.9b).

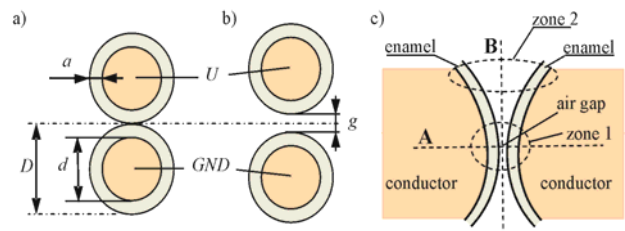


Fig.9. Cross section of the enameled wires in TP sample (insulation thickness not in scale with wire diameter): a) $g = 0$, b) $g > 0$, c) PD zones in insulating system of TP sample

The conditions for PD inception are determined by the electric field distribution between the wires. Without PD it

can be approximated by capacitive field distribution, which is formed by a series of two capacitances of dielectric layer of insulation. When PDs are present, one can assume that the air space due to ionization starts to be conductive.

Corona-like discharge is the mechanism of PD initiation between two insulated wires. Thus, the PD inception voltage U_i depends on the wire's diameter in TP samples. At 50 Hz sinusoidal voltages the PD φ - q - n patterns can be acquired and analyzed [1]. The PD intensity, described by the total number of PD pulses $N(U)$ is shown in Figure 10.

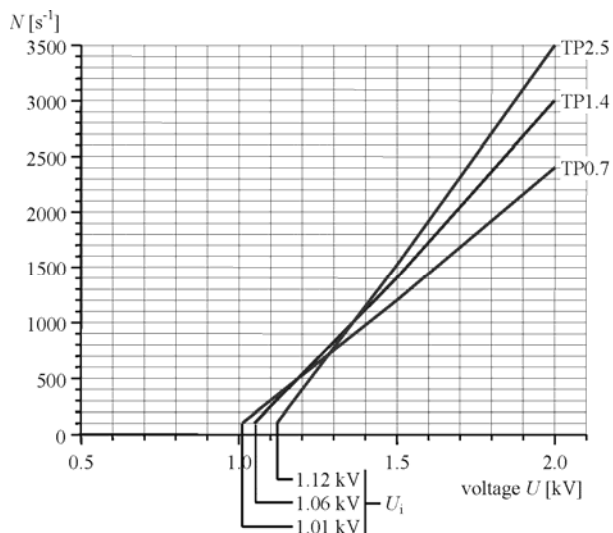


Fig.10. The number of PD pulses N vs. voltage U for TP samples made from wires with 0.7 mm, 1.4 mm, and 2.5 mm diameter

Analysis of electric field distributions in elements of motor windings

The wound wires in TP samples create an insulating system with solid dielectric (coatings of enameled wires) or with micro-gap g between them. Along the TP sample, there are many distributed contact points of adjacent wires, which are in close proximity separated only by a micro gap in air. During the PD measurements the TP samples are exposed to the electric field higher than PD inception field. Electric field distribution in TP sample depends on: wire diameter D , insulation thickness a , number of twists ts , and airgap g between wires. For investigations of PD initiation and development in TP insulation systems, the two zones have been distinguished (Fig.9c):

- **Zone 1:** micro-air gap exists at the contact of insulated wires, which form the insulation system composed of serial dielectrics. In this zone the electric field distribution is approximately uniform, therefore only normal electric field components occur. Their values are high in the air gap and much lower in the solid dielectric. The reason is that dielectric stress is reversely proportional to dielectric constant ϵ_r , the value of which is 3.8 – 4.2.
- **Zone 2:** boundary region, adjacent to the contact point. Apart from regular electric field components also tangential components occur there.

The electric field calculations along the profile A and B (Fig.9c) provide information about those field components. The distribution of electric field in insulating systems represented by twisted-pair model samples is directly connected with the mechanism of inception and development of partial discharges and electric breakdown.

In parallel configuration of wires in TP sample no twists occur ($ts = 0$). One can considerate two cases:

- without air gap between the wires $g = 0$,
- the air gap exists, $g = 100 \mu\text{m}$.

a) No distance between wires $g = 0$ mm

The electric field distribution for parallel, adjoin wires for exemplary TP0.7 sample at 1 kV is presented in Figure 11.

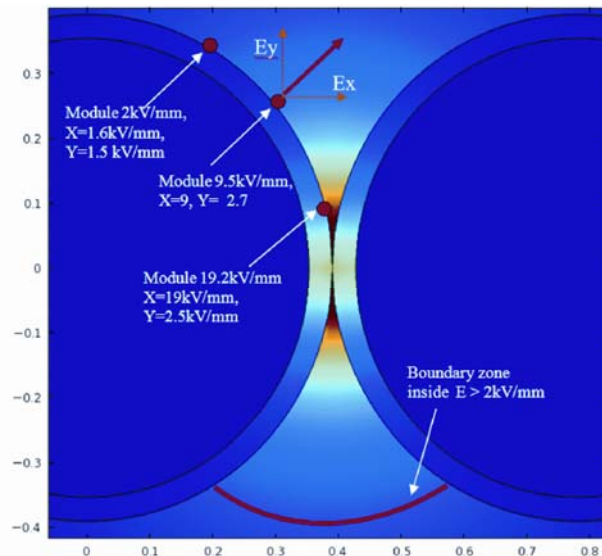


Fig.11. Electric field for parallel wires without air gap ($g = 0$)

The electric field is depicted in three characteristic spots, one in the region of highest field near the contact point of wires, the second one in the region of strong electric field ($E = 9.5 \text{ kV/mm}$) and the third one on the boundary region, where the electric field drops below 2 kV/mm . The electric field in the cross sections of the wire's contact point, along A and B profiles depicted in Figure 9c, is shown in plot in Figure 12. A high electric field of $30 - 40 \text{ kV/mm}$ exists in the micro-air gap between wires and exceeds approx. 9 kV/mm corona inception stress characteristic for 0.1 mm gap. The diameter of wires in the twisted pair samples is particularly influencing the electric field distribution in the non-homogenous areas in twisted pair sample (Fig.12b).

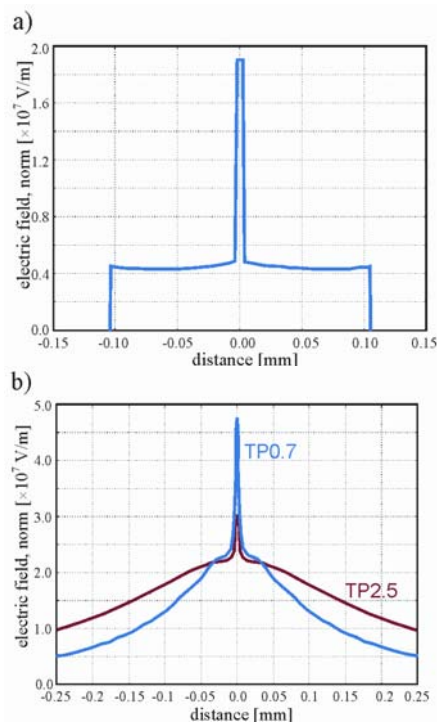


Fig.12. Electric field distribution along: a) profile A for TP0.7 and TP2.5, b) profile B for TP0.7 and TP2.5 [1]

b) Distance between wires $g = 100 \mu\text{m}$

The electric field distribution for parallel wires placed in the proximity $g = 100 \mu\text{m}$ at 1 kV is presented in Figure 13. In such a way a micro-air gap is formed between wires.

Similarly like for adjacent wires, also in case of air slice, the electric field is depicted in three characteristic spots, one in the region of highest field, the second one in the region of moderate electric field ($E = 4 \text{ kV/mm}$) and the third one on the boundary region, where the electric field drops below 2 kV/mm .

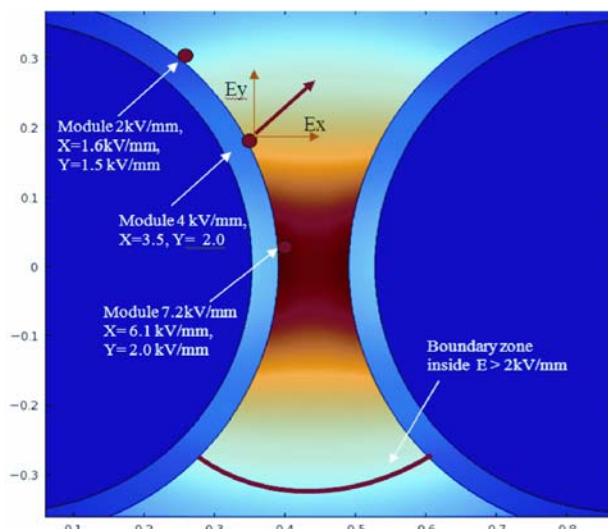


Fig.13. Electric field for parallel wires with air gap ($g = 100 \mu\text{m}$)

Results of simulations show characteristic regions with significantly different values of electric field. These conditions influence the development of partial discharge forms, which can be indirectly confirmed by microscopic observation of the surface of wires insulation (Fig.14). It refers to the need of development a special wires design with higher resistance to fast surges [10, 13, 14].

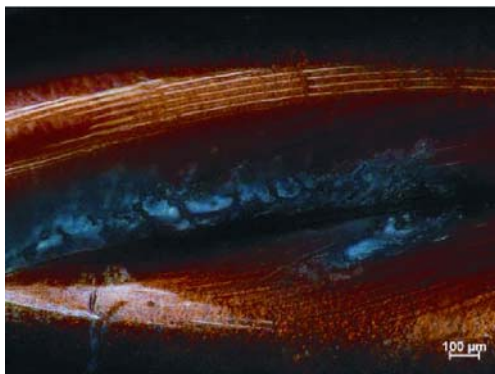


Fig.14. Microphotographs of twisted wires from TP sample with insulation deterioration traces and breakdown hotspot

Conclusions

Partial discharge measurement is sensitive tool for assessment of winding wires quality and properties of new insulating materials.

In motor windings, represented here by twisted-pair samples, partial discharges may occur in air gaps with

a width from several μm up to tens of μm , at the inception voltage from approximately 850 V to 1400 V [10].

Modern methods of pulse signals detection and acquisition help us in better understanding of physical processes leading to inception and development of partial discharges in motor winding insulation. Numerical analysis of electric fields with modelling of real, imperfect configurations of winding wires pointed out possible ways of impulsive degradation processes of their insulating layers.

The development of an enamelled wire that can withstand coil winding stress increases the reliability of electric motors fed by inverters.

REFERENCES

- [1] Florkowska B., Zydroń P., Florkowski M.: Effects of converter pulses on the electrical insulation system of motors, *Proc. 2011 IEEE ISIE*, 573 – 578, Gdańsk, 2011
- [2] IEC/TS 60034-18-41 ed. 1 (2006-10): Rotating electrical machines – Part 18-41: Qualification and type tests for Type I electrical insulation systems used in rotating electrical machines fed from voltage converters
- [3] Bonnet A. et al: Cause and analysis of stator and rotor failures in three phase squirrel cage induction motors, *IEEE Trans. IAS*, vol. 1992, 921 – 937
- [4] Persson E.: Transient effects in applications of PWM inverters in induction motors, *IEEE Trans. IAS*, vol. 1992, 1095-1101
- [5] IEC 60851-5 ed. 4.0 (2008-07): Winding wires. Test methods – Part 5: Electrical properties
- [6] IEC 60172 ed. 3.0: Test procedure for the determination of the temperature index of enamelled winding wires
- [7] Florkowska B., Florkowski M., Zydroń P., Roehrich J., Pędzisz K.: Degradation processes of polymer cable insulation at non-sinusoidal voltage stresses, *Conf. Rec. 2010 IEEE ISEI*, San Diego, CA, USA, paper 132
- [8] Lindell E., Bengtsson T., Blennow J., Gubanski S.M., Influence of rise time on partial discharge extinction voltage at semi-square voltage waveforms, *IEEE Trans. Dielectr. Electr. Insul.*, vol. 17, no. 1, 2010, 141–148
- [9] Cavallini A., Montanari G.C.: Effect of supply voltage frequency on testing of insulation system, *IEEE Trans. Dielectr. Electr. Insul.*, vol. 13, no. 1, 2006, 11 – 21
- [10] Florkowska B., Florkowski M., Furgat J., Roehrich J., Zydroń P, Impact of fast transient phenomena on electrical insulation systems, AGH-UST Press; Kraków, 2012
- [11] IEC-60270 ed. 3, (2000-12) High-voltage test techniques – Partial discharge measurements
- [12] IEC/TS 61934 ed. 2.0 (2011-04): Electrical insulating materials and systems – Electrical measurement of partial discharges (PD) under short rise time and repetitive voltage impulses
- [13] Manh Quan Nguyen ; Malec D., Mary D., Werynski P., Gornicka B., Therese L., Guillot, P., Silica nanofilled varnish designed for electrical insulation of low voltage inverter-fed motors, *IEEE Trans. Dielectr. Electr. Insul.*, vol. 17, no. 5, 2010, 1349–1356
- [14] Glinka T., Kulesz B.: Wyładowania niezupełne w izolacji zwojowej silników indukcyjnych zasilanych z falowników PWM, *Prace Naukowe Instytutu Maszyn, Napędów i Pomiarów Elektrycznych Politechniki Wrocławskiej*, Nr 49, Studia i Materiały Nr 21, 2000

Authors:

Barbara Florkowska, Prof., E-mail: beflor@agh.edu.pl; Józef Roehrich PhD EE, E-mail: roehrich@agh.edu.pl; Paweł Zydroń PhD, D.Sc. AGH University of Science and Technology, Dept. of Electrical and Power Engineering, Mickiewicza 30, 30-059, Krakow, Poland, E-mail: pzydron@agh.edu.pl; Marek Florkowski PhD D.Sc., ABB Corporate Research Center, Starowiślna 13A, 31-038 Krakow, Poland, E-mail: marek.florkowski@pl.abb.com.